Article

Not peer-reviewed version

A Deep Learning Framework with Intermediate Layer using Swarm Intelligence Optimizer for diagnosing Oral Squamous Cell Carcinoma

Bharanidharan Nagarajan , Sannasi Chakravarthy S R , Vinoth Kumar V , Mahesh T R * , Surbhi Bhatia Khan *

Posted Date: 6 October 2023

doi: 10.20944/preprints202310.0290.v1

Keywords: oral cancer; histopathologic images; CNN; deep learning framework; swarm

Article

A Deep Learning Framework with Intermediate Layer using Swarm Intelligence Optimizer for Diagnosing Oral Squamous Cell Carcinoma

Bharanidharan Nagarajan [1], Sannasi Chakravarthy [2], Vinothkumar Venkatesan [3], Mahesh Thyluru Ramakrishna [4] and Surbhi Bhatia Khan [5],*

[1,3] School of Computer Science Engineering and Information Systems, Vellore Institute of Technology, Vellore, India bharanidharan.n@vit.ac.in; drvinothkumar03@gmail.com

[2] Department of ECE, Bannari Amman Institute of Technology, Sathyamangalam, India; sannasi@bitsathy.ac.in

[4.] Department of Computer Science and Engineering, Faculty of Engineering and Technology, JAIN (Deemed-to-be University), Bangalore, 562112, India; trmahesh.1978@gmail.com

[5] Department of Data Science, School of Science Engineering and environment, University of Salford, Manchester United Kingdom; surbhibhatia1988@yahoo.com

* Correspondence: Author: Surbhi Bhatia Khan (surbhibhatia1988@yahoo.com)

Abstract: Oral Squamous Cell Carcinoma is one among the most common cancer and early detection is the main key to avoid deaths. Automated diagnostic tools that process the histopathological images of a patient to detect abnormal oral lesions will be very much useful for the clinicians. A deep learning framework have been designed with an intermediate layer between feature extraction layers and classification layers for classifying the histopathological images into two categories, namely normal and oral squamous cell carcinoma. The intermediate layer is constructed using the proposed Swarm Intelligence technique called Modified Gorilla Troops Optimizer. Various optimization algorithms are implemented in literature for optimal parameter identification, weights updating and feature selection in deep learning models, but this work focuses on usage of optimization algorithm as intermediate layer that transforms the extracted features into the features that are more suitable for classification. Three datasets totally comprising 2784 normal and 3632 oral squamous cell carcinoma subjects are considered in this work. Three popular CNN architectures namely InceptionV2, MobileNetV3, and EfficientNetB3 are investigated as feature extraction layers. Two fully connected Neural Network layers along with batch normalization and dropout are used as classification layers. Among the investigated feature extraction models, MobileNetV3 performs well in all the three datasets with the highest accuracy of 0.89. Usage of the proposed Modified Gorilla Troops Optimizer as an intermediate layer boosts this accuracy to 0.95.

Keywords: oral cancer; histopathologic images; CNN; deep learning framework; swarm intelligence; gorilla troops optimizer

1. Introduction

Any neighbour tissue impairment due to uncontrolled cell growth and its invasion is called as Cancer. Oral cancer is ranked sixth most prevailing cancer globally and it falls under the broad category of head and neck cancer. Oral cancer results in malignant cancer cell growth in lips and various parts of oral cavity. Worldwide, it is ranked as the fifteenth most common reason for death among various types of cancer. Out of one lakh people, minimum four people are affected by this disease across the globe [1,2]. Approximately, seventy-seven new cases and fifty-two thousand deaths are registered every year in India and one-fourth of the global oral cancer occurs in India [3].

Most common types of oral cancer include Oral Squamous Cell Carcinoma (OSCC), Verrucous carcinoma, Minor salivary gland carcinomas, Lymphoma, and Mucosal melanoma. Among them, OSCC is a predominant type of oral cancer which contributes around 84% – 97% of oral cancer [4]. The major risk factors that lead to development of OSCC includes tobacco usage, frequent chewing of betel quid, alcohol intake, oral infection, and genetic disorders [5]. Detection of OSCC at early stage is very crucial to avoid deaths since the five-year survival rate of humans with early-stage OSCC is around 85% while it is only around 40% with advanced stage [6,7]. Hence early detection is the key to reduce the mortality rate and so there is a huge demand for diagnostic tools that identifies the OSCC at earlier stages of malignancy.

Apart from physical examination, major diagnostic tools used for identification of oral cancer includes techniques such as endoscope biopsy, liquid biopsy, vital staining technique, ultrasound imaging, Magnetic Resonance Imaging (MRI), Computed Tomography (CT) imaging, Raman spectroscopy, Gene/DNA array-based biomarker detection, enzyme assays-based biomarker detection, and histopathological examination [4]. Among these techniques, histopathologic examination is mainly preferred since it can be used to detect both malignant and benign tumours by identifying the changes in histopathological and molecular levels. Histological assays can be used to reveal the gradual growth of malignant cells in oral cavity beginning from elementary dysplasia to tumours with high invasive nature. It is helpful in analysing the cells proliferation, growth of abnormalities, cytoplasmic-level and cellular-level atypia, changes at the surface of epithelium, and deep tissue-level cytoarchitecture [8]. Usually, abnormalities in microscopic and clinical levels arise only after the abnormalities in molecular and genetic levels. Histopathological examination is good in capturing these molecular level changes and so preferred for early detection [9].

Analysis of histopathological images through visual inspection is usually subjective in nature and prone to errors sometimes. Computerized diagnostic tools will be very helpful to assist the clinician in the decision-making process to reduce such errors. Various Machine Learning (ML) techniques are used nowadays in variety of fields. Particularly in healthcare field, the implementation of ML algorithms is increasing day by day. Accuracy and robustness are the key concerns in such healthcare related decision-making tools. Fortunately, nowadays Deep Learning (DL) models are available for solving these issues. Deep learning is a sub-field in machine learning where the Artificial Neural Network (ANN) models with many numbers hidden layers are trained with large set of training images and labels; labels of new unseen images will be predicted using the trained model. The main advantage of deep learning is the non-requirement of hand-crafted feature engineering compared to traditional supervised classifiers such as Support Vector Machine (SVM), K-Nearest Neighbour (KNN), Decision Trees (DT), etc where domain experts are required to identify the appropriate features and Region of Interest (RoI) [10,11].

Convolutional Neural Network (CNN) is a popular deep learning technique where convolution operation is involved in multiple ANN layers. Various CNN architectures are developed, and they are very efficient in different image classification tasks [12,13]. Popular CNN architectures include ResNet, EffiecientNet, InceptionNet, MobileNet, etc. The main advantage of these architectures is their ability to work well on a classification task even if most of their weights are pre-trained on another classification task. This concept is known as transfer learning and works very well for two similar and unique classification tasks. Two main advantages of transfer learning are reduction in training time and competence to work well on small datasets [14,15].

To improve the accuracy of such deep learning models, various techniques are used such as fine-tuning, feature selection, regularization, optimal parameter selection, optimization, etc. On the other hand, various population-based Swarm Intelligence (SI) optimization algorithms are widely used for optimal parameter identification, weights updating and feature selection in deep learning models for enhancing the accuracy. SI algorithms are meta-heuristic iterative algorithm that are usually inspired by the characteristic and nature of Swarm of animals. These algorithms are preferred in many applications mainly due to their minimalism, derivation free design and ability to avoid local optima [16]. Some of the popular SI algorithms include Particle Swarm Optimization (PSO), Ant Colony Optimization, Grey Wolf Optimizer, Dragonfly Optimization, Elephant Herding Optimization, Gorilla Troops Optimizer (GTO), etc.

This work primarily focuses on classifying the histopathological images into two categories: Normal and OSCC. Histopathological image features are extracted using pre-trained weights of transfer learning based popular CNN models namely InceptionV2, MobileNetV3, and

EfficientNetB3. Then Modified Gorilla Troops Optimizer (MGTO) is used as an intermediate layer in between feature extraction and classification layers. Two fully connected ANN layers along with batch normalization and dropout are used as classification layers.

The key contributions of this research work are listed below:

1. Proposal of novel deep learning framework that includes a swarm intelligence-based optimization algorithm as an intermediate layer in deep learning model.
2. Development of MGTO through appropriate modifications that enhances the classification accuracy.
3. Comparative analysis of popular deep learning models with and without the proposed intermediate layer in terms of various classification metrics and training time.

The remaining paper is organized as follows: Section 2 deals with the related works and section 3 is related to background of various transfer learning models used and original GTO. Fourth section deals with the methodology used in this research work and fifth section presents the implementation procedure for proposed MGTO as an intermediate layer. Results are presented and discussed in the sixth section. Last section summarizes the conclusion and future work.

2. Related work

Various techniques based on machine learning and deep learning are proposed in the literature to diagnose oral cancer by analysing the medical images. Early publication related to oral cancer diagnosis mainly revolves around feature extraction and traditional supervised classifiers [17-20]. For example, [21] considered features based on texture discrimination using higher order spectra, laws texture energy, and local binary pattern and fed these features to supervised classifiers such as DT, Gaussian Mixture Mode, KNN, Sugeno Fuzzy Classifier, and Radial Basis Probabilistic Neural Network. Similarly, [22] proposed textural changes detection using features extracted from digital images of oral lesions through grey level cooccurrence matrix and grey level run length matrix. They used back propagation-based ANN for classification. Particularly for OSCC diagnosis, [23,24] proposed texture, shape and colour feature extraction from histopathological images and classification through DT, SVM, and Logistic Regression.

Usage of deep learning models in medical image analysis is increasing rapidly particularly from the last decade onwards. Various deep learning models are developed and tested for oral cancer diagnosis that involves both binary and multi-class classification. [25] investigated customized AlexNet to detect OSCC from histopathological images. [26] investigated DenseNet121 model on oral biopsy images to detect OSCC and found that it performs better than Regions with CNN (R-CNN) model. Other transfer learning models such as Inception-ResNet-V2 [27], Xception [28], ResNet101 [29] are also investigated for diagnosing oral cancer from medical images. Apart from the above-mentioned works where popular CNN architectures are investigated, some works are reported which proposes their own CNN model for detecting oral cancer. For example, [30] proposed HRNet model for diagnosing malignant lesions in oral cavities and compared it with popular ResNet50 and DenseNet169 models. [31] developed a modified CNN model which performs well when compared to transfer learning-based models such as Resnet-50, VGG-16, VGG-19, and Alexnet. Similarly, [29] proposed their own ten-layer CNN model that outperforms the pretrained CNN models in diagnosis of OSCC from histopathological images. Other than CNN and its variants, capsule networks are also implemented in some works to identify oral malignancy. [32] tested the performance capsule networks to identify OSCC from histopathological images.

To increase the classification accuracy and robustness of deep learning models, various optimization algorithms are investigated in many applications and some of them are summarized as follows: [33] designed a hybrid optimization algorithm that mixes PSO and Al-Biruni Earth Radius Optimization for optimizing the design parameters of CNN and Deep Belief Network in malignant oral lesion identification. [34] presented segmenting psoriasis skin images using Adaptive Golden Eagle Optimization for finding the ideal weight and bias parameters of CNN. [35] considered Artificial Bee

Colony optimization algorithm for finding the optimal hyper-parameters of CNN that works as classifier for identifying the species of plant. [36] proposed optimal guidance-whale optimization algorithm to select features extracted from AlexNet–ResNet50 model and supplied the selected features to Bi-directional long short-term memory for Land Use Land Cover classification. [37] suggested Modified Lion Optimization for selecting the optimal features for transfer learning-based CNN classification model to build a multimodal biometric system. In this manner, numerous optimization algorithms are incorporated for finding optimal hyper-parameters, training the model, and feature selection in deep learning. Comparatively only few works are reported regarding the usage of optimization algorithm as a transformation technique. For example, crow search optimization algorithm is used as transformation technique for improving the classification performance of weighted KNN in severity classification of breast cancer [38].

From the above related works, the following points can be summarized. Compared to hand crafted feature extraction and traditional supervised classifiers, deep learning models perform well in diagnosis of OSCC. But still, they are lagging in classification accuracy and robustness. To solve those two concerns, optimization algorithms are widely used in various applications for improvisation of deep learning models in different ways. Hence this work attempts to use MGTO optimization algorithm as an intermediate layer between feature extraction and classification layers for enhancing the accuracy of OSCC diagnosis.

3. Background

3.1. CNN

CNN [39] based deep learning models are widely used to classify images in variety of applications mainly due to their capability of recognizing the underlying pattern. Convolution operation at multiple layers act as the foundation for CNN and generally a typical CNN contains convolutional layers, pooling layers and fully connected layers. The goal of convolution layers is to extract the image attributes such as contours, colours, etc. Pooling layers will act as a dimensionality reduction layer i.e., it reduces the number of features. Max and average pooling layers are very popular when compared to others. The last stage is usually built using fully connected layers called DenseNet and it is responsible for classification [40].

3.2. InceptionV2

Inception [41] model is an altered version of CNN in which inception blocks are included. These inception blocks refer to the processing of same input with different filter sizes before combining them. InceptionV2 is an advanced variant of original InceptionV1. When compared to Inception V1, two 3*3 convolution operations are performed in InceptionV2 instead of one 5*5 convolution operation. In addition, filter size n*n is factorized into 1*n and n*1 convolutions in Inception V2.

3.3. MobileNetV3

MobileNet [42] is a modified version of CNN where batch normalization and ReLU activation functions are used instead of single 3*3 convolution layer. In addition, one convolution operation is carried out for each colour channel in MobileNet while flattening of colour channels will happen in typical CNN. Relatively MobileNet architectures requires minimal computational power and so mainly preferred in mobile devices and embedded systems. Compared to MobileNetV1, bottleneck with residuals are implemented in MobileNetV2 while layer removal and swish non-linearity are incorporated in MobileNetV3.

3.4. EfficientNetB3

Unlike typical CNN, EfficientNet [43] uniformly scales all dimensions with a compound coefficient. Fixed set of scaling coefficients are used to uniformly scale the network depth, width and resolution. The original EfficientNetB0 version is based on the MobileNetV2 combined with squeeze and excitation blocks. EffientNetB3 is developed by scaling up baseline network of previous versions.

3.5. Gorilla Troops Optimization

GTO is one of the iterative meta-heuristic optimization algorithms which is proposed in the year 2021 [44]. It is based on the social activities and characteristics of Gorilla troop. Usually, each such troop contains one adult male gorilla which is called as silverback gorilla, substantial number of adult female gorillas, and their Childs. The male gorilla will lead the troop and it is responsible for controlling the troop activities such as identification of sources of food, solving the conflicts, and decision making. GTO is mathematically modelled as five-stage algorithm where three stages are responsible for exploration while the remaining two stages are related to exploitation. The positions of Gorillas are updated using the following equations:

$$X(t+1) = \begin{cases} (U_l - L_l) * r_1 + L_l & rand < p \\ (r_2 - C) * X_r(t) + L * H & rand \geq 0.5 \\ X(t) - L * (L * (X(t) - X_r(t)) + r_3 * (X(t) - X_r(t))) & rand < 0.5 \end{cases} \quad (1)$$

Here X is the position of current Gorilla at iteration t. r_1, r_2, r_3 and $rand$ are the random numbers in the range 0 to 1. p is a parameter whose value will usually lie between 0 and 1. U_l and L_l are the upper and lower boundaries respectively. X_r is a Gorilla randomly chosen at each iteration. The values of C, L, and H are calculated using the equations (2), (4), and (5) respectively.

$$C = F * \left(1 - \frac{Iter}{Maxit}\right) \quad (2)$$

$$F = \cos(2 * r_4) + 1 \quad (3)$$

$$L = C * l \quad (4)$$

$$H = Z * X(t) \quad (5)$$

In equation (2), $Iter$ represents the current iteration and $Maxit$ represents the maximum number of iterations. F present in equation (2) is calculated using equation (3) and r_4 is a random number in the range 0 to 1. Here l is an integer randomly chosen in the range -1 to 1. In equation (5), Z is a random number in the range -C to +C. Based on the position of Silverback, other gorillas will change their position while searching for food and this behaviour is represented using the equation (6). The M value mentioned in equation (6) is computed using the equations (7) and (8).

$$X(t+1) = L * M * (X(t) - X_{silverback}) + X(t) \quad (6)$$

$$M = \left(\left|\frac{1}{N}\sum_{i=1}^{N} X_i(t)\right|^g\right)^{\frac{1}{g}} \quad (7)$$

$$g = 2^L \quad (8)$$

Here $X_{silverback}$ is the position of Silverback Gorilla which is the Gorilla with best position when compared to positions of other Gorillas and N is the total number of Gorillas. Gorillas' behaviour for competing to choose the adult females is represented using the equation (9).

$$X(t+1) = X_{silverback} - (X_{silverback} * Q - X(t) * Q) * A \quad (9)$$

$$Q = 2 * r_5 - 1 \quad (10)$$

$$A = \beta * E \quad (11)$$

$$E = \begin{cases} N_1 & rand \geq 0.5 \\ N_2 & rand < 0.5 \end{cases} \quad (12)$$

In the above equations, r_5 and $rand$ are the random numbers in the range 0 to 1 while β is a parameter whose value is crucial in deciding the updated positions of Gorillas. N_1 is a random number in the range decided by the problem dimension while N_2 is a random number that follows normal distribution in the range [0,1]. Initially, equation (1) will be used to update all the Gorilla's position. Then Silverback Gorilla will be found in that iteration. After that, other Gorillas position will be updated based on Silverback Gorilla's position. If the value of $|C| \geq 1$, then the position of Gorillas is updated using equation (6) otherwise they will be updated using equation (9).

3.6. Particle Swarm Optimization

PSO [45] is one of the popular and efficient swarm intelligence-based optimization algorithm. PSO is inspired from the characteristics exhibited by bird flocks while searching for food. Usually, the population will be initialized randomly and updated in each iteration based on the fitness function. The velocity of each particle is mathematically modelled and updated using equation (13).

$$v_i(t+1) = w * v_i(t) + c_1 * r_1 * \left(p_i(t) - x_i(t)\right) + c_2 * r_2 * \left(gbest - x_i(t)\right) \qquad (13)$$

Here, $v_i(t)$ stands for velocity of *i*th particle in iteration *t*; Three crucial parameters PSO are *w*, *c1*, and *c2*; The position of *i*th particle in iteration *t* is represented as $x_i(t)$; $p_i(t)$ and $gbest$ represents the personal best and global best particle positions respectively. r_1 and r_2 are the random number in the range 0 to 1. The position of each particle is updated based old position and new velocity as represented in equation (14).

$$x_i(t+1) = x_i(t) + v_i(t+1) \qquad (14)$$

Personal best and global best will be computed in each iteration using the equations (15) and (16) respectively.

$$p_i(t+1) = \begin{cases} p_i(t) & if\ f\left(x_i(t+1)\right) \geq f\left(p_i(t)\right) \\ x_i(t+1) & if\ f\left(x_i(t+1)\right) < f\left(p_i(t)\right) \end{cases} \qquad (15)$$

$$gbest \in \{p_0(t), p_1(t), \ldots., p_m(t)\} \qquad (16)$$

$$= min\left\{f\left(p_0(t)\right), f\left(p_1(t)\right), \ldots, f(\,p_m(t))\right\}$$

Here, f represents the fitness function which is crucial in deciding the performance of PSO.

3.7. Elephant Herding Optimization

Elephant Herding Optimization (EHO) [46] is inspired by the behaviour of elephants. Like PSO and GTO, EHO also comes under the category of swarm intelligence meta-heuristic algorithm. The position of elephant is updated using equation (17).

$$x_i^{new} = x_i^{old} + \alpha\left(x_{best} - x_i^{old}\right) * ran \qquad (17)$$

Here x_i^{new} and x_i^{old} are the new and old positions of ith elephant. x_{best} is the best elephant position found using equation (18). x_{center} in equation (18) is computed using equation (19). In addition to updating the best elephant position, worst elephant position x_{worst} is also updated using equation (20).

$$x_{best} = \beta * x_{center} \qquad \text{n} \qquad (18)$$

$$x_{center} = \frac{1}{n} * \sum_{i=1}^{n} x_i \qquad (19)$$

$$x_{worst} = x_{min} + (x_{max} - x_{min} + 1) * rand \qquad (20)$$

α and β are the EHO parameters; $rand$ is a random number in the range [0,1]; *n* is the number of elephants. x_{max} and x_{min} are the maximum and minimum boundaries for elephant positions.

4. Materials and Methods

Three publicly available datasets totally comprising 2784 normal and 3632 oral squamous cell carcinoma subjects are considered in this work. First dataset is obtained from Kaggle [45], and it contain oral histopathological images in both 100x and 400x zoom levels. First dataset contains totally 5192 images and out of them 2494 images belong to Normal class and 2698 belongs to OSCC class. Second and third datasets are obtained from the online repository built by Tabassum Yesmin Rahman et al. [46]. Oral histopathological images with zoom levels of 100x and 400x are present in second and third datasets respectively. 89 normal images and 439 OSCC images are available in the second dataset while 201 normal images and 495 OSCC images are available in the third dataset. Some of the sample oral histopathological images belonging to normal and OSCC classes are shown in Figure 1 & Figure 2 respectively.

doi:10.20944/preprints202310.0290.v1

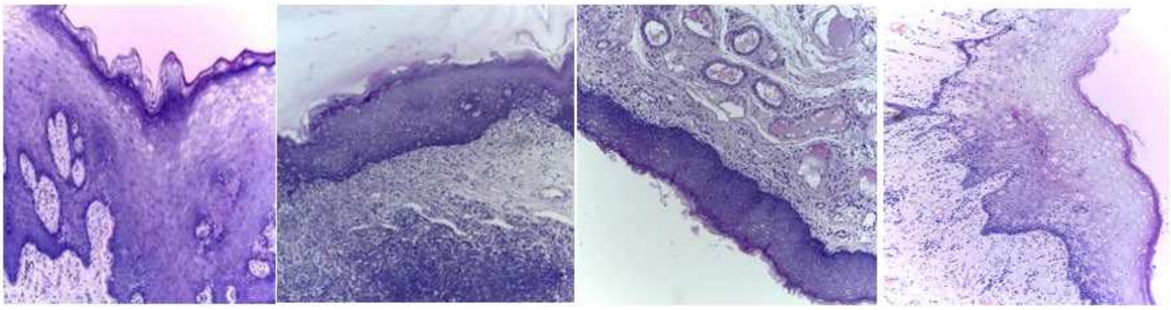

Figure 1. Sample oral histopathological images belonging to Normal class.

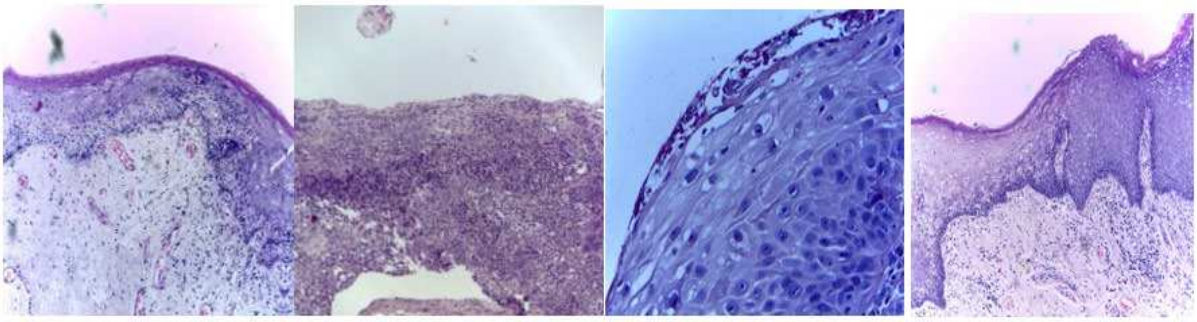

Figure 2. Sample oral histopathological images belonging to OSCC class.

The typical procedure for implementing the oral cancer detection using transfer learning-based feature extraction is shown in Figure 3. Histopathological oral images from the three datasets are fed to the feature extraction layers discretely and resultant classification performance metrics are also computed individually. Features are extracted using the transfer learning approach where the weights are pre-trained for another similar dataset. Three popular CNN architectures namely InceptionV2, MobileNetV3, and EfficientNetB3 are investigated in this work for feature extraction. Weights that are pre-trained for popular ImageNet dataset is considered in all the three architectures. The extracted features are then divided into training, validation, and test feature sets using stratified shuffle split approach in the 70:15:15 ratio respectively. Stratified shuffle split is considered since it randomly selects the samples according to the class ratio in the original dataset. In other words, stratified shuffle split ensures the ratio of each class in all the three resultant sets as same as shown in Table 1. This approach of data splitting is very crucial in imbalanced datasets. Then the classification layers are trained using training and validation feature sets where the ideal weights of neural networks for classifying the oral histopathological images are found.

Two fully connected Neural Network layers along with batch normalization and dropout are used as classification layers as shown in Figure 4. Finally, the trained classification layers with ideal weights are used to classify the test feature set as Normal or OSCC class. In Figure 4, the functional layer depicts the transfer learning based pre-trained model while the remaining layers are used for classification. The specifications of classification layer considered in this research work is presented in Table 2. For comparison purposes, the classification layer is unaltered for all the datasets and different feature extraction layers. Specifications related to number of epochs and batch size during training, optimizer, early stopping and reduction of learning rate on plateau are also mentioned in Table 2. Based on the transfer model used for feature extraction layer, the number of trainable parameters of complete deep learning model will vary as shown in Table 3. The number of features extracted per input image by the three different feature extraction layers are also shown in Table 3.

Table 1. Stratified shuffle data split on three datasets.

Dataset	Class	Total number of samples	Number of training samples	Number of validation samples	Number of test samples
First	Normal	2494	1746	374	374
	OSCC	2698	1890	404	404
Second	Normal	89	63	13	13
	OSCC	439	307	66	66
Third	Normal	201	141	30	30
	OSCC	495	347	74	74

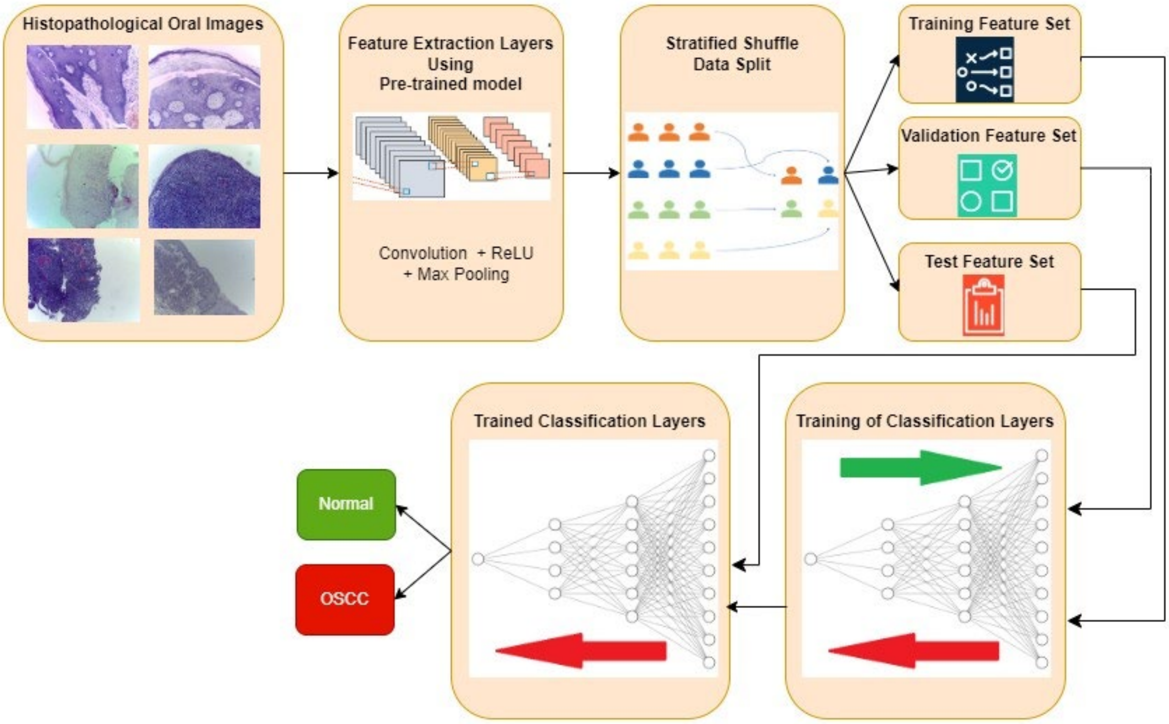
Histopathological Oral Images
Feature Extraction Layers Using Pre-trained model
Convolution + ReLU + Max Pooling
Stratified Shuffle Data Split
Training Feature Set
Validation Feature Set
Test Feature Set
Trained Classification Layers
Training of Classification Layers
Normal
OSCC

Figure 3. Typical approach for OSCC detection using Transfer learning-based feature extraction.

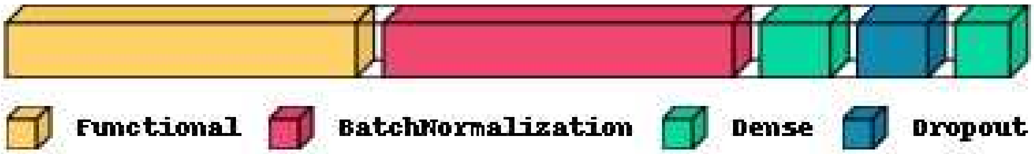

Figure 4. Typical deep learning architecture with functional layer depicting the transfer learning model for feature extraction and remaining layers depicting the classification layers.

Table 2. Specifications of classification layer and techniques used.

Classification layers & techniques used	Specifications
Batch Normalization	momentum= 0.99, epsilon= 0.001
Dense	units = 256, kernel regularizer = L2 regularizer with coefficient l = 0.016, activity regularizer = L1 regularizer with coefficient l = 0.006, bias regularizer = L1 regularizer with coefficient l = 0.006, activation= ReLu
Dropout	drop rate= 0.45
Dense	units = 2, activation= SoftMax

Training	epochs = 100, batch size = 128, stratified shuffle split: training - 70%, testing - 15%, validation -15%
Optimizer	Adamax with learning rate= 0.001, loss= sparse categorical cross-entropy, metrics=accuracy
Early stopping	patience = 5, minimum delta = 0, monitor = validation loss, restore best weights = True, mode = minimum
Reduce learning rate on Plateau	monitor = validation loss, factor = 0.2, patience = 4, mode = minimum

Table 3. Specifications of Feature extraction layer.

Feature extraction Layers	Total number of parameters	Number of Trainable parameters	Number of features extracted
Mobilenet V3	25,91,554	3,31,010	1280
Efficientnet B3	1,11,83,665	3,97,058	1536
InceptionV2	5,47,36,866	3,97,058	1536

The proposed approach for OSCC detection is presented in Figures 5 and 6. An intermediate layer based on MGTO is included in the proposed method when compared to Figure 3 and Figure 4. Like classification layer, the newly introduced intermediate layer also needs to be trained where it will learn the ideal values for its parameters related to the MGTO algorithm. Hence it will be trained with original training and validation feature sets. Then all the three original feature sets will be supplied as input to the trained MGTO layer where the features sets are transformed to produce another three transformed sets namely training, testing, and validation. The size of the input and output feature sets remains same. Then the transformed sets are considered for classification layers for detecting the class of oral histopathological image. This research work is carried out in a system with following configurations: i9 processor with 32GB RAM and NVIDIA RTX A2000 12GB GPU.

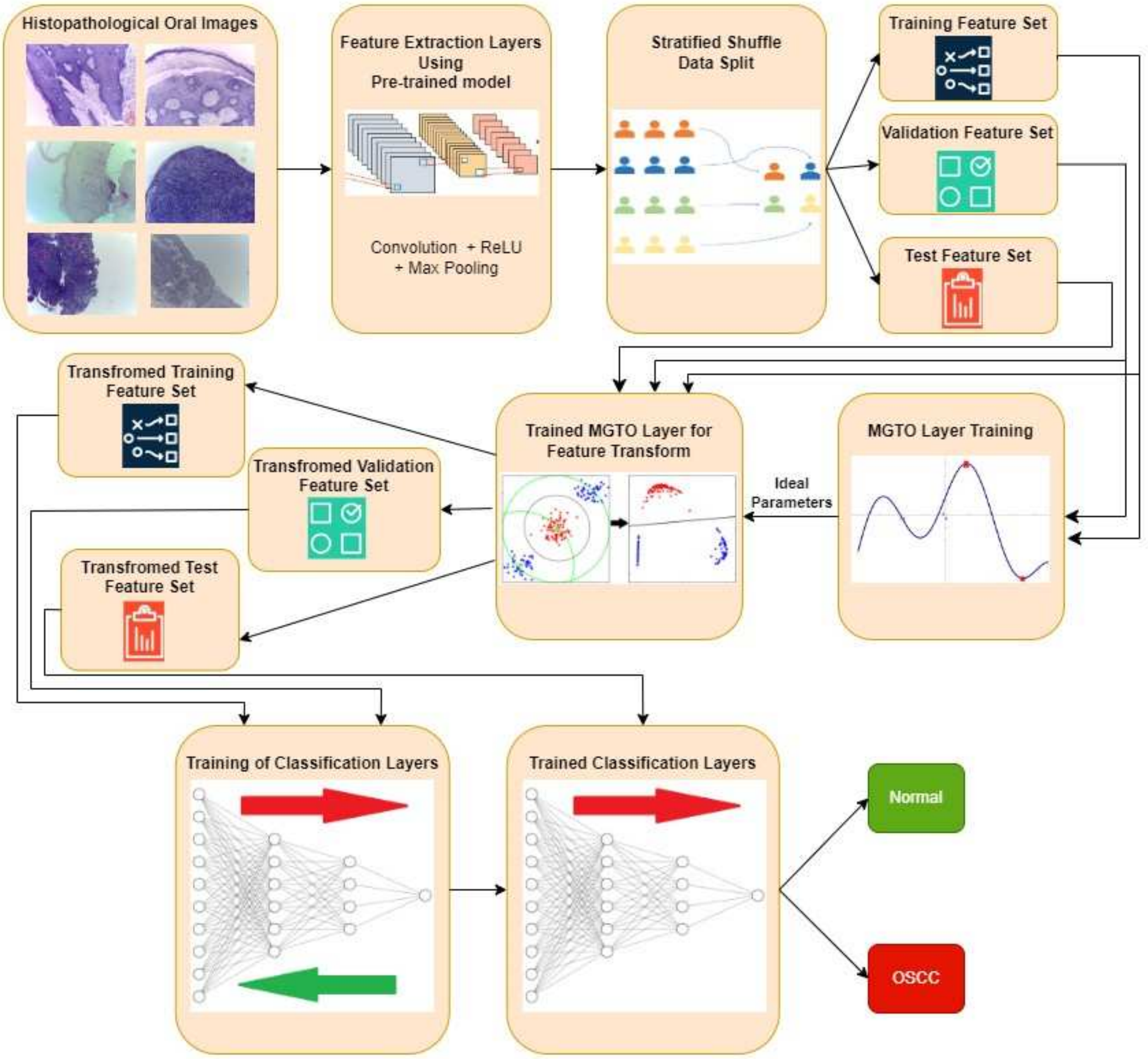
Histopathological Oral Images
Feature Extraction Layers Using Pre-trained model
Convolution + ReLU + Max Pooling
Stratified Shuffle Data Split
Training Feature Set
Validation Feature Set
Test Feature Set
Transfromed Training Feature Set
Transfromed Validation Feature Set
Transfromed Test Feature Set
Trained MGTO Layer for Feature Transform
Ideal Parameters
MGTO Layer Training
Training of Classification Layers
Trained Classification Layers
Normal
OSCC

Figure 5. Overview of Proposed Approach for OSCC Detection.

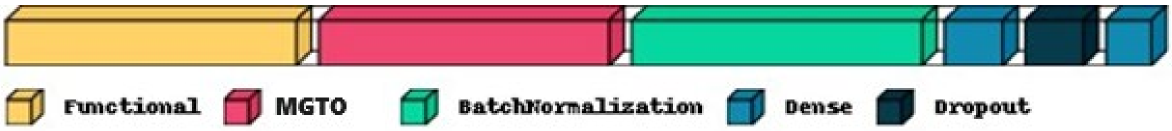

Figure 6. Proposed deep learning architecture where MGTO is used as intermediate layer between feature extraction (functional) layer and classification layer. .

5. Implementation of Proposed MGTO

The equations to update the Gorilla's position are modified based on Sine Cosine Algorithm [48] to increase the exploitation and exploration capabilities of GTO. In MGTO, three equations that update the position of Gorillas are modified. Equations (1), (6), and (9) of GTO are modified as represented in equations (21), (22), and (23) respectively in MGTO. All other equations of GTO remain intact in MGTO.

$$X(t+1) = \begin{cases} (U_l - L_l) * r_1 + L_l & rand < p \\ (r_2 - C) * X_r(t) + L * H & rand \geq 0.5 \\ X(t) - L * rad * sin\big(X(t) - X_r(t)\big) + rad * cos(X(t) - X_r(t))) & rand < 0.5 \end{cases} \quad (21)$$

$$X(t+1) = L * M * rad * sin(X(t) - X_{silverback}) + X(t) \quad (22)$$

$$X(t+1) = X_{silverback} - rad * cos(X_{silverback} * Q - X(t) * Q) * A \quad (23)$$

rad in the above equations is computed using equation (24). const in equation (24) is a constant and it is considered as three as suggested in [48]; Crnt_ Iter represents the current iteration number while Max_Iter represents the maximum number of iterations.

$$\mathrm{rad} = \mathrm{const} - \mathrm{Crnt\ \ Iter} \times \left(\frac{\mathrm{const}}{\mathrm{Max}_{\mathrm{Iter}}}\right) \quad (24)$$

original GTO, the Gorilla's population is initialized randomly. But to use MGTO as intermediate layer in deep learning models, the Gorilla's population is initialized with the features extracted from the previous layer. Number of Gorillas will be equal to the number of features extracted. Then the Gorilla's position will be updated in each iteration using MGTO equations. Fitness function is very crucial in optimization algorithms, and it will be selected based on the problem to be solved. To use MGTO for transforming the features, the fitness function based on variance metric is considered. Fitness of each Gorilla, $\mathrm{F}(X_i)$ will depend on its own position and four nearest-neighbour Gorillas as shown in equation (25).

$$\mathrm{F}(X_i) = \mathrm{Variance}(X_{i-2}, X_{i-1}, X_i, X_{i+1}, X_{i+2}) \quad (25)$$

In MGTO, p and β are the parameters which mainly decides the performance along with Max_Iter. The ideal values of these parameters are found based on the accuracy attained during training and validation. Validation accuracy for various values of Max_Iter is plotted in Figures 7 and 11 is found as ideal value where the validation accuracy of 0.77 is reached. While finding the optimal value for Max_Iter, other two parameters namely p and β are kept as 0.5 (median of range [0,1]). To find the optimal values for p and β parameters, Max_Iter is kept at its ideal value 11. Figure 8 depicts the validation accuracy for various values of p and β parameters. Highest validation accuracy of 0.95 is attained when p =0.3 and β =0.7. Finding the ideal values for the parameters of MGTO is termed as training and for this purpose, training and validation feature sets are used. After training, MGTO transform will be implemented for all the three feature sets namely training, validation, and test sets with the ideal parameters value of Max_Iter = 11, p =0.3, and β =0.7. Notably these are the ideal parameters of MGTO on first dataset when MobileNetV3 is employed as feature extraction layer. The ideal parametric values may change depending upon the input data given to MGTO layer. The ideal values for other input data will be presented in the next section. Procedure for implementing the MGTO as intermediate feature transform layer for test feature set is summarized in Algorithm 1.

Algorithm 1: Algorithm to implement the proposed MGTO as intermediate layer in deep learning models for feature transformation of test feature set.

Step 1: Extract features using pre-trained transfer learning models for each oral histopathological image.

Step 2: Consider number of features as size of population in MGTO. Initialize the position of Gorillas with extracted features.

Step 3: Initialize parameters of MGTO: $U_l = \max\,(X^1, X^2, \dots., X^N)$, $L_l = \min\,(X^1, X^2, \dots., X^N)$, $\mathrm{Max}_{\mathrm{Iter}} = 11$, p =0.3, and β =0.7

Step 4: Compute the fitness value of each Gorilla using equation (25)

Step 5: Update the position of each Gorilla using equation (21)

Step 6: Identify the Silverback Gorilla i.e., the Gorilla with highest fitness.

Step 7: Update the position of each Gorilla using equation (22) if $|C| \geq 1$. Otherwise use equation (23)

Step 8: Repeat steps 4 to 7 until maximum number of iterations is reached. If the maximum number of iterations are completed, then go to step 9.

Step 9: Consider the final position of Gorillas as the output of Feature Transform and give them as input to the classification layer.

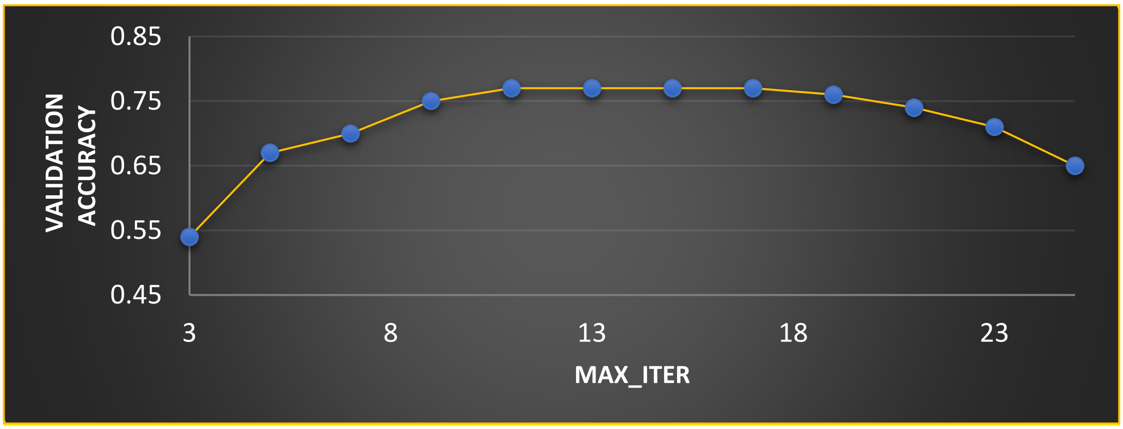

Figure 7. Ideal value computation for Max_Iter.

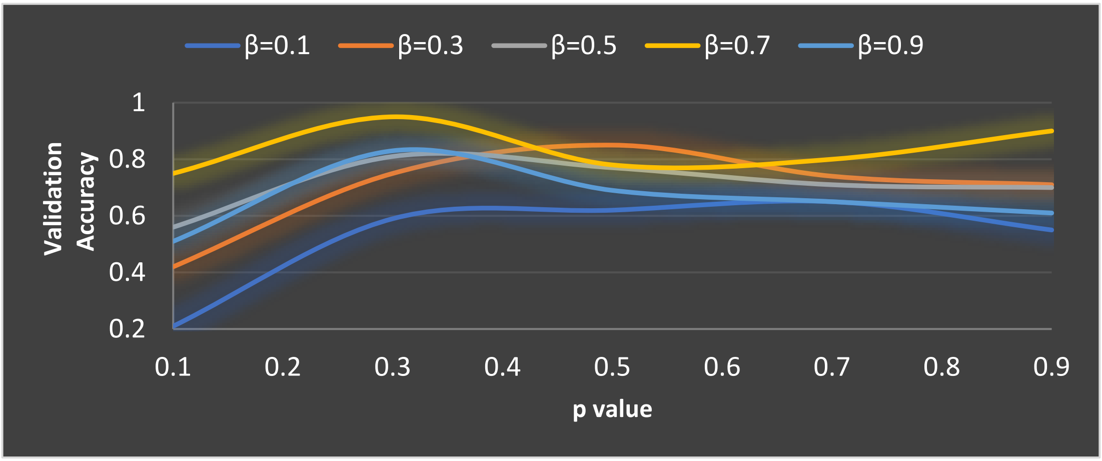

Figure 8. Ideal value computation of p and β parameters.

6. Results and Discussion

Initially the experiment is conducted without any intermediate layer in the deep learning model. Three different transfer learning-based models namely InceptionV2, MobileNetV3, and EfficientNetB3 are tested as feature extraction layers. As mentioned in Table 2, the specifications of classification layer remain the same for all the three different feature extraction layers. The confusion matrix attained for these three deep learning models without intermediate layer on first dataset in OSCC detection is shown in Figure 9. The label 0 represents the class Normal and label 1 represents the class OSCC in Figure 9. EfficientNetB3 classify all the input images as OSCC and so its True Negative (TN) = 0. This clearly indicates the poor performance of the EfficientNetB3 based deep learning model without intermediate layer. To detect OSCC, high TP is required while to detect normal class properly, high TN is required. Among the remaining two models without intermediate layer, highest True Positive (TP) is attained by MobileNetV3 while the highest TN is attained by InceptionV2.

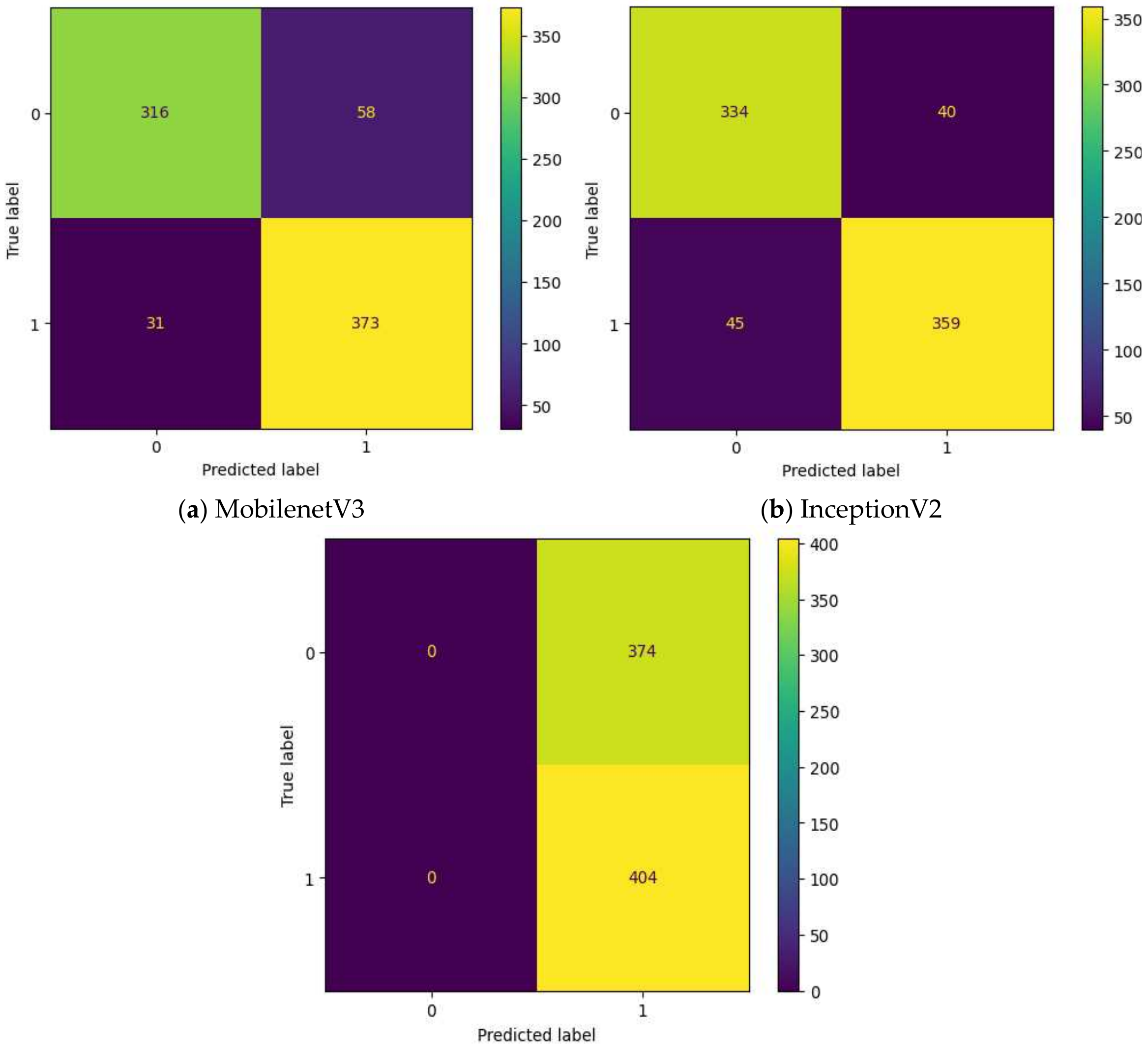

(**a**) MobilenetV3 (**b**) InceptionV2

(**c**) EfficientnetB3.

Figure 9. Confusion Matrix of Deep learning models without intermediate layer.

To improve the number of TN and TP, MGTO based intermediate layer is proposed in this work. Figure 10. shows the confusion matrix of three different feature extraction-based deep learning models with MGTO as intermediate layer in OSCC detection. When MGTO is not used as intermediate layer in EfficientNetB3 based deep learning model, then all the oral images are classified as OSCC while better TN and TP values are attained with the proposed layer. Highest TN and TP values are attained for the proposed MobileNetV3 based feature extraction with MGTO as intermediate layer.

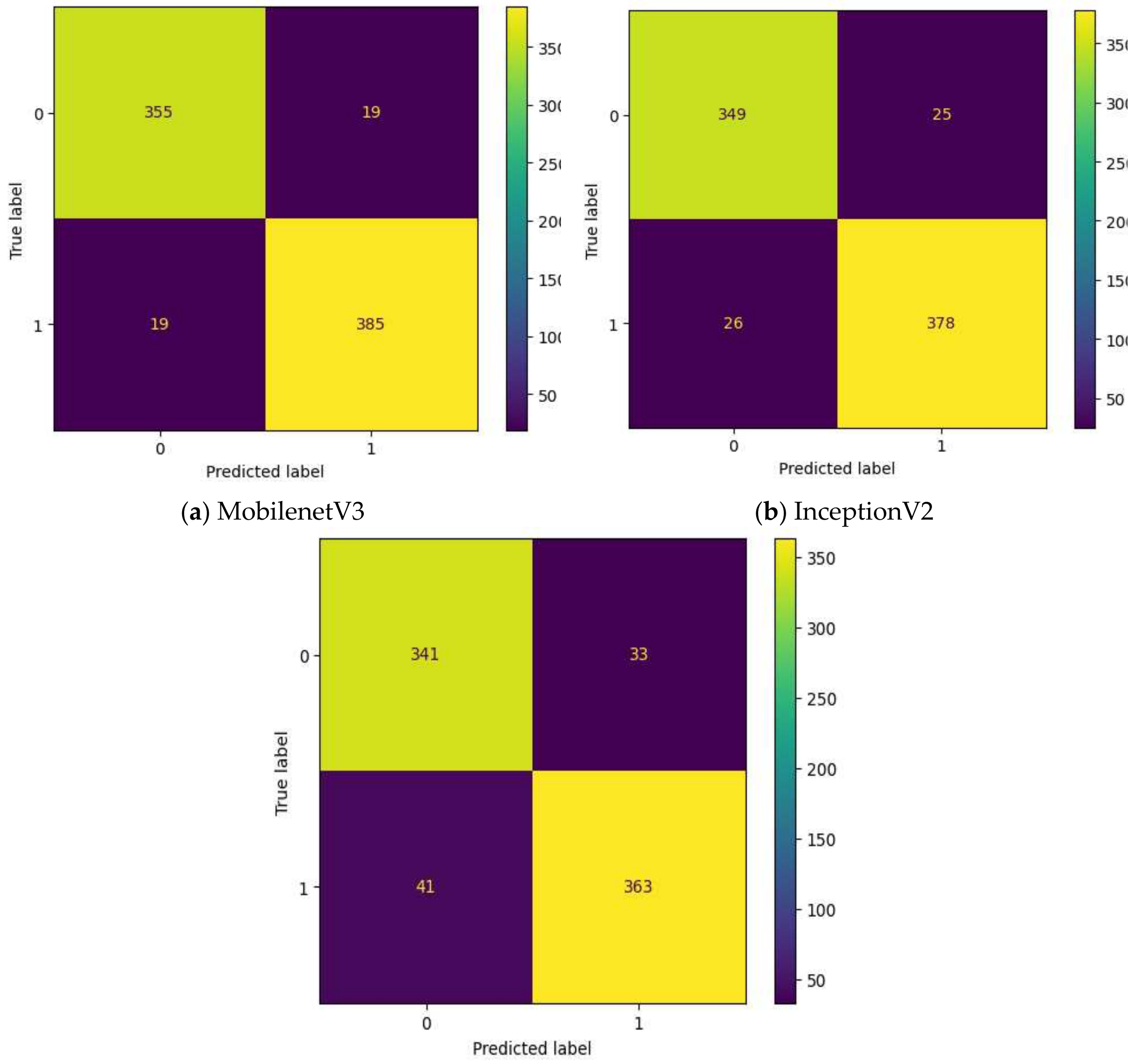

(**a**) MobilenetV3

(**b**) InceptionV2

(**c**) EfficientnetB3

Figure 10. Confusion Matrix of Deep learning models with MGTO as intermediate layer.

Based on the confusion matrix, four popular performance metrics namely Accuracy, Precision, Recall, and F1-score are used in this research work to analyse the performance of deep learning models. Apart from deep learning models with and without MGTO based intermediate layer, three other swarm intelligence-based optimization algorithms namely PSO, EHO, and GTO are also tested as intermediate layer and their results are also presented in Table 4. Implementation procedure for PSO, EHO, and GTO as intermediate layer will also follow the Algorithm 1 presented in previous section. Only the parameters and the way of updating the position of Swarm will vary based on the optimization algorithm used. The final ideal parameters of all the four tested intermediate layer after training is listed in Table 5.

Table 4. Performance metrics computed on test set of first dataset.

Transfer learning model	Intermediate layer	Accuracy	Precision	Recall	F1-score
MobilenetV3	NO	0.89	0.87	0.92	0.89
EfficientnetB3	NO	0.52	0.52	1	0.68
InceptionV2	NO	0.88	0.89	0.88	0.88
MobilenetV3	PSO	0.79	0.78	0.82	0.8

EfficientnetB3	PSO	0.75	0.75	0.78	0.77
InceptionV2	PSO	0.82	0.85	0.8	0.82
MobilenetV3	EHO	0.77	0.77	0.8	0.79
EfficientnetB3	EHO	0.8	0.82	0.78	0.8
InceptionV2	EHO	0.83	0.85	0.82	0.83
MobilenetV3	GTO	0.87	0.87	0.88	0.88
EfficientnetB3	GTO	0.81	0.83	0.8	0.81
InceptionV2	GTO	0.86	0.86	0.88	0.87
MobilenetV3	MGTO	0.95	0.95	0.95	0.95
EfficientnetB3	MGTO	0.9	0.92	0.9	0.91
InceptionV2	MGTO	0.93	0.93	0.93	0.93

Table 5. Ideal parameters of various intermediate layers.

Feature extraction	Intermediate layer	Ideal Parameter values
MobilenetV3	PSO	Max_Iter = 10, w=0.6, c1=0.7, and c2=0.9
	EHO	Max_Iter = 12, α = 0.9, and β=0.8
	GTO	Max_Iter = 11, p = 0.2, and β = 0.7
	MGTO	Max_Iter = 11, p = 0.3, and β = 0.7
EfficientnetB3	PSO	Max_Iter = 12, w=0.4, c1=0.7, and c2=0.9
	EHO	Max_Iter = 12, α = 0.7, and β=0.8
	GTO	Max_Iter = 8, p = 0.5, and β = 0.7
	MGTO	Max_Iter = 9, p = 0.3, and β = 0.8
InceptionV2	PSO	Max_Iter = 12, w=0.6, c1=0.8, and c2=0.8
	EHO	Max_Iter = 11, α = 0.8, and β=0.6
	GTO	Max_Iter = 7, p = 0.4, and β = 0.7
	MGTO	Max_Iter = 9, p = 0.4, and β = 0.6

The main objective of this work is to detect OSCC and so precision, recall, and F1-score in Table 4 are related to truthful identification of OSCC class while the accuracy metric is related to truthful identification of both normal and OSCC classes. As seen in Table 4, deep learning models without any intermediate layer provides less accuracy than the proposed deep learning models with MGTO as intermediate layer.

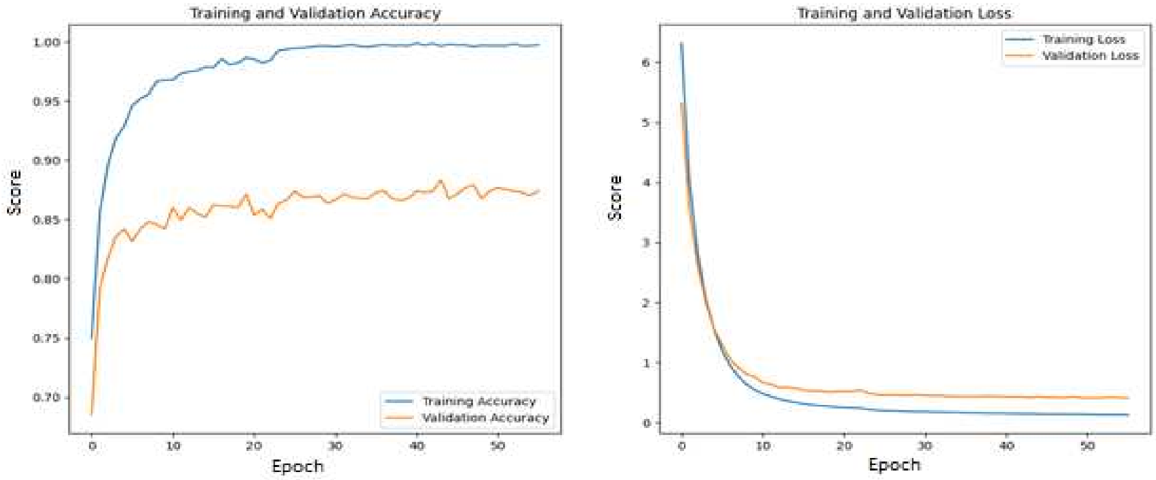

(**a**) MobilenetV3

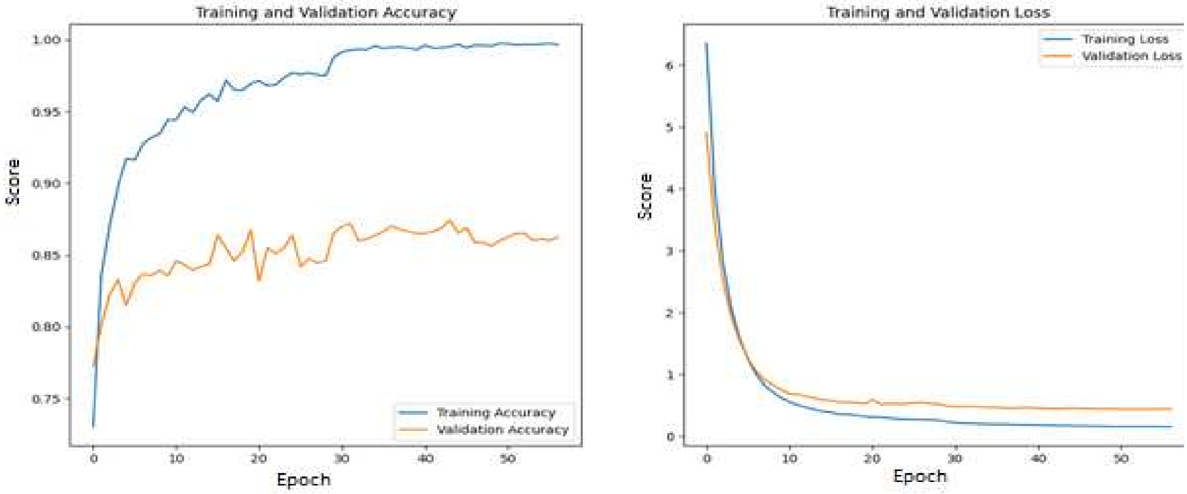

(**b**) InceptionV2

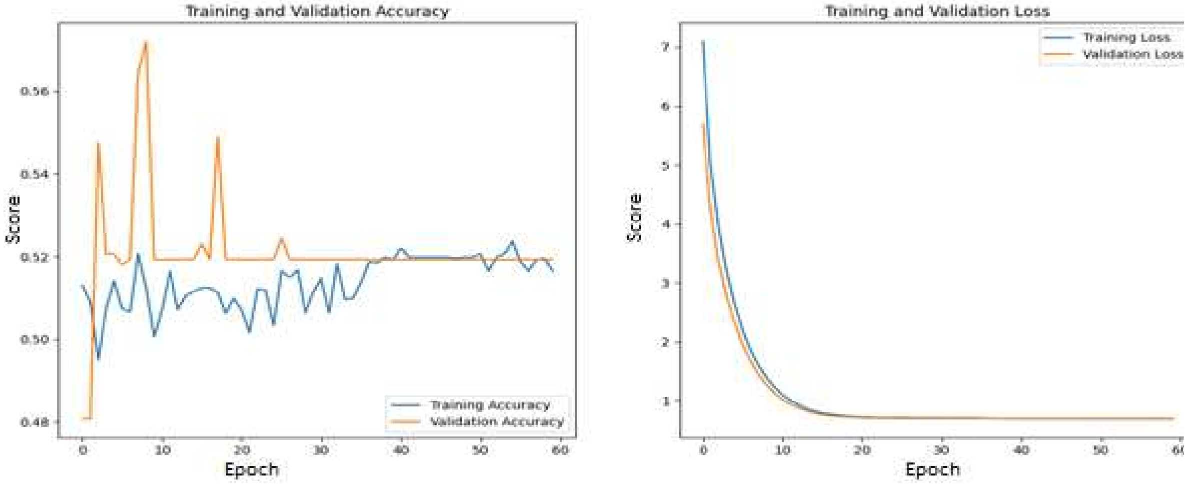

(**c**) EfficientnetB3

Figure 11. Training & validation accuracy and loss of Deep learning models without intermediate layer on first dataset.

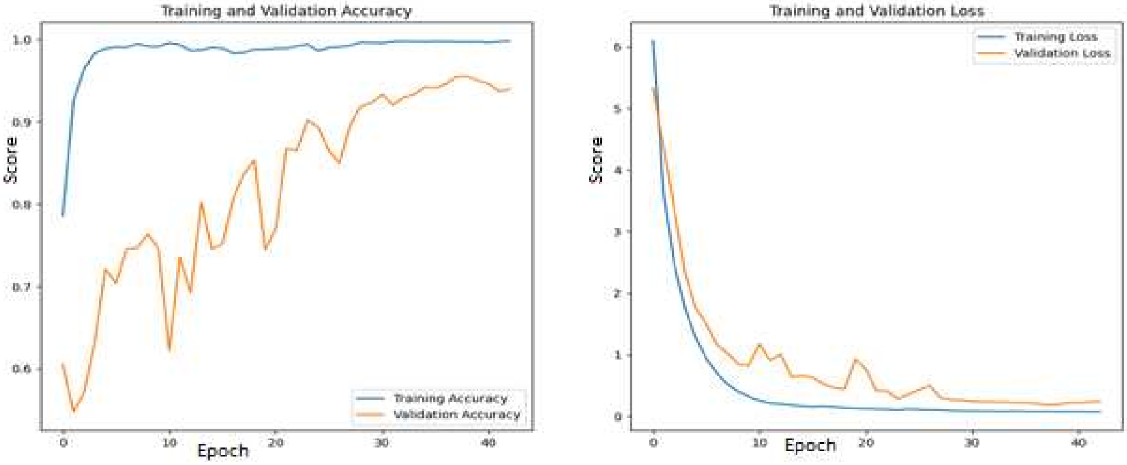

(**a**) MobilenetV3

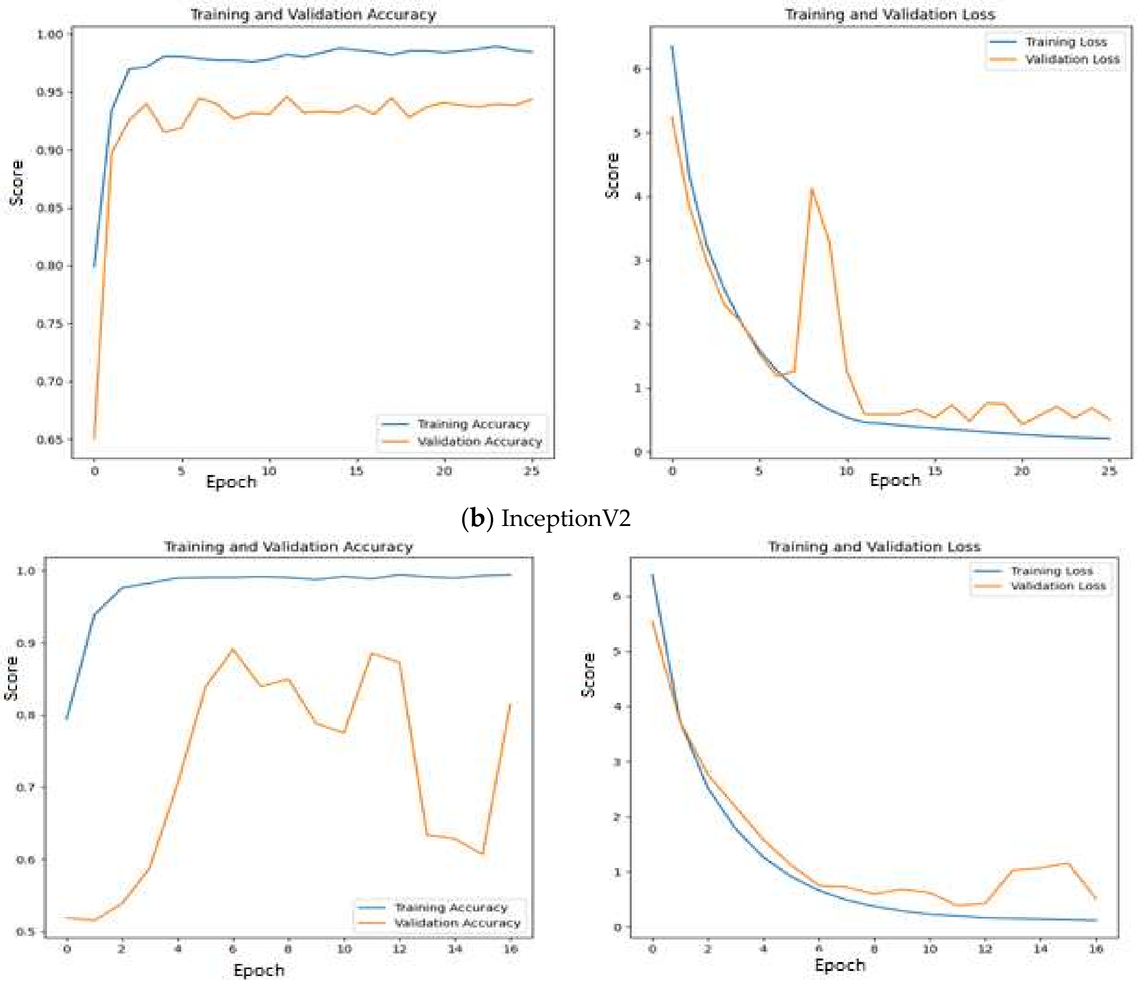

(**b**) InceptionV2

(**c**) EfficientnetB3

Figure 12. Training & validation accuracy and loss of Deep learning models with MGTO as intermediate layer on first dataset.

Among the models without intermediate layer, MobileNetV3 offers highest accuracy of 0.89 which is followed by InceptionV2 with accuracy of 0.88 and EfficientNetB3 with accuracy of 0.52. The reason for such poor performance of EfficientNetB3 is explained as follows: All the three feature extraction models are pre-trained on ImageNet dataset and features are extracted based on the weights appropriate for ImageNet dataset. The weights and architecture of EfficientNetB3 fails to capture the significant features from input oral images while vital features are properly extracted by the remaining two feature extraction models. This statement is further supported by Figure 11 where the training and validation accuracy & loss are presented for all the three investigated deep learning models without intermediate layer on the first dataset.

Since quality features are extracted by MobileNetV3 and InceptionV2, both training & validation accuracy are increasing gradually during training. In addition, both training & validation loss are also decreasing in exponential manner. But deep learning model that uses EfficientNetB3 fails to grow both training and validation accuracy due to poor features extracted from the histopathological oral images. Figure 12 presents the training & validation accuracy and loss when MGTO is used as intermediate layer on the first dataset. It clearly shows the improved accuracy during both training and validation because of transformed appropriate features produced by MGTO. To support the findings based on first dataset, other two smaller OSCC datasets are tested. The second and third dataset are highly imbalanced since the number of OSCC class samples is much higher than the number of normal class samples. The performance metrics attained on those two datasets are presented in Table 6 and Table 7.

Table 6. Performance metrics computed on test set of second dataset.

Transfer learning model	Intermediate layer	Accuracy	Precision	Recall	F1-score
MobilenetV3	NO	0.8	0.8	0.97	0.88
EfficientnetB3	NO	0.74	0.74	1	0.85
InceptionV2	NO	0.8	0.82	0.93	0.87
MobilenetV3	PSO	0.78	0.81	0.92	0.86
EfficientnetB3	PSO	0.75	0.79	0.9	0.84
InceptionV2	PSO	0.8	0.81	0.95	0.87
MobilenetV3	EHO	0.76	0.8	0.9	0.85
EfficientnetB3	EHO	0.75	0.81	0.86	0.84
InceptionV2	EHO	0.78	0.82	0.9	0.85
MobilenetV3	GTO	0.82	0.82	0.98	0.89
EfficientnetB3	GTO	0.78	0.81	0.92	0.86
InceptionV2	GTO	0.82	0.83	0.97	0.89
MobilenetV3	MGTO	0.88	0.88	0.97	0.92
EfficientnetB3	MGTO	0.81	0.81	0.97	0.88
InceptionV2	MGTO	0.86	0.84	1	0.91

Table 7. Performance metrics computed on test set of third dataset.

Transfer learning model	Intermediate layer	Accuracy	Precision	Recall	F1-score
MobilenetV3	NO	0.84	0.86	0.92	0.89
EfficientnetB3	NO	0.71	0.71	1	0.83
InceptionV2	NO	0.82	0.86	0.89	0.88
MobilenetV3	PSO	0.78	0.84	0.85	0.85
EfficientnetB3	PSO	0.73	0.81	0.81	0.81
InceptionV2	PSO	0.78	0.83	0.87	0.85
MobilenetV3	EHO	0.8	0.84	0.89	0.86
EfficientnetB3	EHO	0.73	0.81	0.83	0.82
InceptionV2	EHO	0.81	0.85	0.89	0.87
MobilenetV3	GTO	0.91	0.92	0.96	0.94
EfficientnetB3	GTO	0.75	0.83	0.83	0.83
InceptionV2	GTO	0.86	0.87	0.95	0.9
MobilenetV3	MGTO	0.94	0.97	0.85	0.96
EfficientnetB3	MGTO	0.9	0.93	0.93	0.93
InceptionV2	MGTO	0.93	0.97	0.93	0.95

From the Table 4, Table 6, and Table 7, it is very clear that MGTO works very well as intermediate layer when compared to other tested intermediate layers in all the three datasets. The significance of MGTO as intermediate layer can be clearly witnessed in Figure 13 where percentage of accuracy increase attained by the usage of various intermediate layers when compared to deep learning model without intermediate layer is depicted.

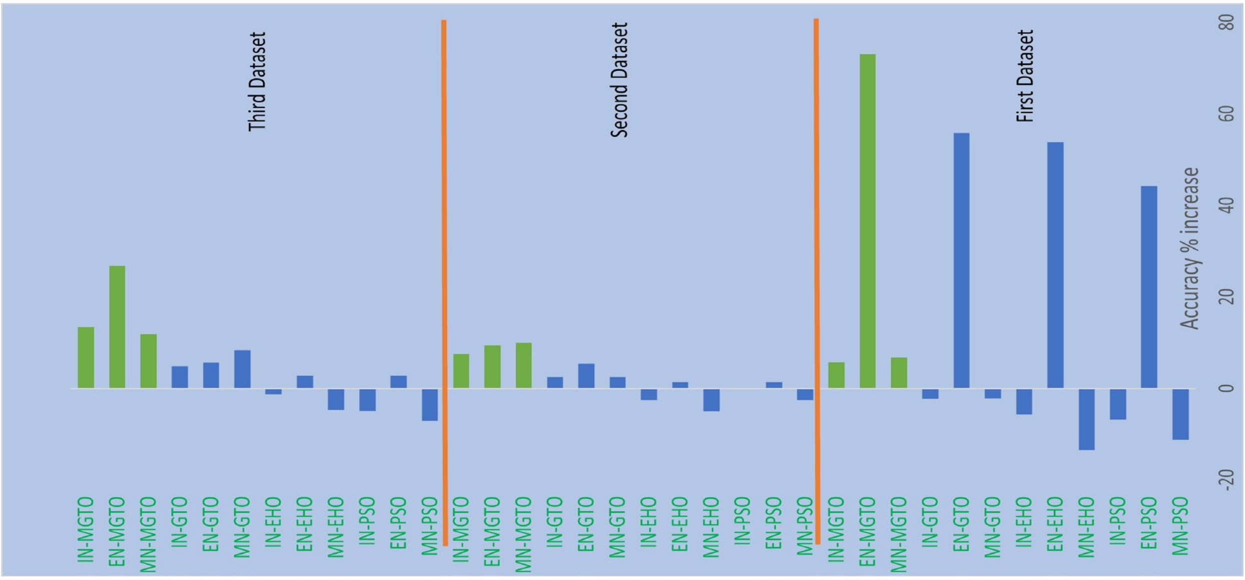

Figure 13. Percentage accuracy increase due to the usage of intermediate layers in DL models when compared to the accuracy offered by DL models without intermediate layer.

On all the three datasets, the percentage of accuracy increase is very less or even negative when PSO, EHO, & GTO are used as intermediate layer on the features extracted from MobileNetV3 and InceptionNetV2. Notably, already these two feature extraction models without intermediate layer produces accuracy of more than 0.8 in all the three datasets. Implicitly, these intermediate layers fails to significantly improve the accuracy since they are not able to produce more appropriate transformed features for classification. Only on the features extracted by EfficientNetB3 of first dataset, these intermediate layers are able to provide significant accuracy increase since the original features extracted by EfficientNetB3 is very poor on the first dataset which yield accuracy of only 0.52. Out of these three intermediate layers, GTO comparatively performs well on all the three datasets. Hence intuition for improving GTO further with suitable modifications raised. MGTO is formulated with the modifications stated in the previous section and it worked well on all the three datasets.

In the first dataset, 73% of increase in accuracy is witnessed on the EfficientNetB3 based DL model due to the usage of MGTO as intermediate layer. Nearly 6% accuracy is increased due to MGTO on MobileNetV3 and InceptionV2 based DL models. Notably the highest accuracy 0.95 is produced on the first dataset by MobileNetV3-MGTO based DL model. Even on the imbalanced second and third datasets, MGTO is capable of producing significant accuracy increase. The reason for this better performance is threefold. Firstly, the modification of GTO with Sine and Cosine algorithm increases its exploration and exploitation capability well. Exploitation is responsible for local search i.e., fine-tuning and exploration is responsible for global search. Secondly, the selection of appropriate fitness function. Local variance based fitness function worked well to transform the features of different classes in different way. Thirdly, the usage of ideal parameters in MGTO resulted in better accuracy. As shown in Figure 7 & Figure 8, values of MGTO parameters will have huge impact on accuracy. Due to the above mentioned reasons, MGTO works soundly as intermediate layer that transforms the input features into more-appropriate features for classification. In other words, the introduction of proposed intermediate layer helps the classifier to distinguish the features of two different classes. This statement is backed by the scatter plots shown in Figure 14, Figure 15, and Figure 16. In scatter plots, the label 0 represents the class Normal and label 1 represents the class OSCC. To represent the features of first dataset in scatter plot, two averages are computed. Average1 is the mean of first half features and Average2 is the mean of remaining half features. For example, 1280 features are extracted by MobileNetV3; mean of first 640 features are considered as Average1 and remaining 640 features are considered as Average2.

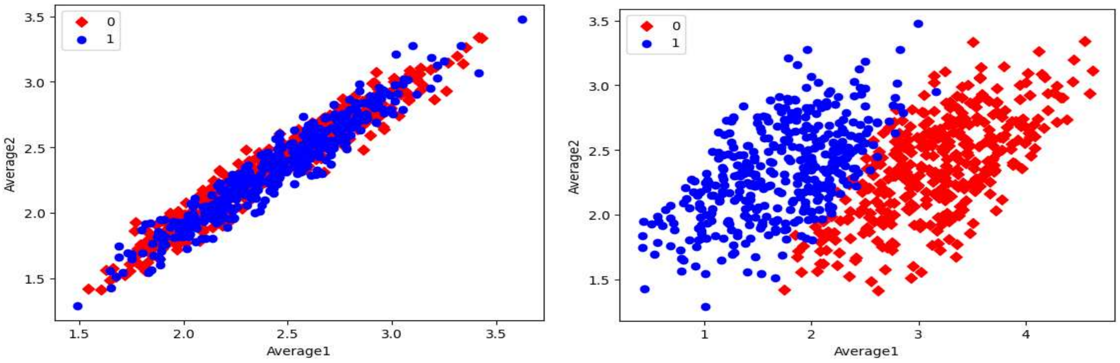

(**a**) without intermediate layer (**b**) with MGTO as intermediate layer

Figure 14. Scatter Plot of features extracted by MobileNetV3.

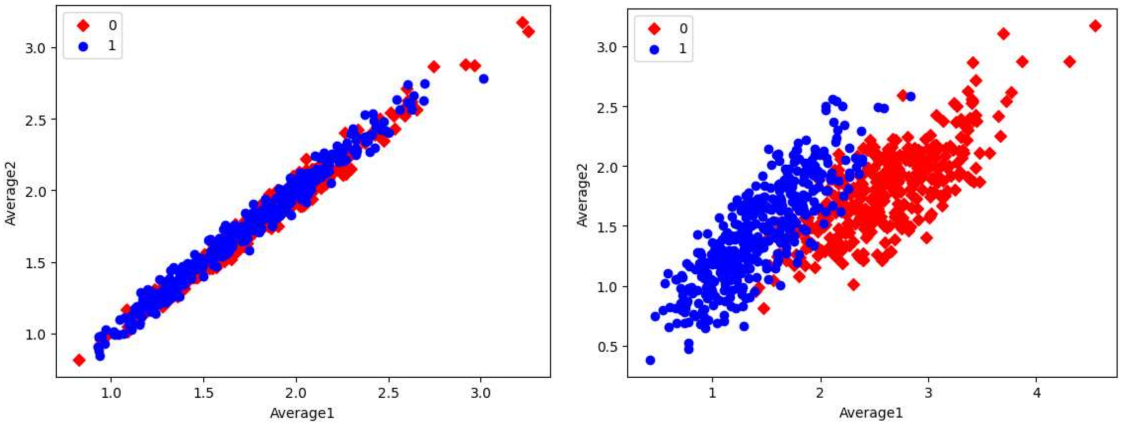

(**a**) without intermediate layer (**b**) with MGTO as intermediate layer

Figure 15. Scatter Plot of features extracted by InceptioNetV2.

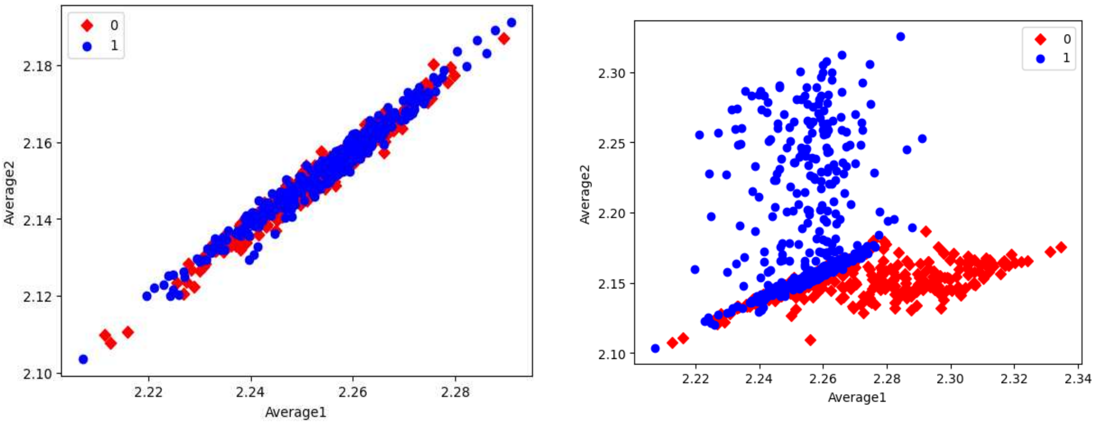

(**a**) without intermediate layer (**b**) with MGTO as intermediate layer

Figure 16. Scatter Plot of features extracted by EfficientNetB3.

Comparison of three scatter plots without intermediate layer, gives the reasons for better performance of MobileNetV3 and poor performance of EfficientNetB3. MobileNetV3 features of two classes are slightly scatter and overlapped while EfficientNetB3 features are heavily overlapped. On comparison of scatter plots with and without intermediate layers of all the three feature extraction models, clearly suggests the significance of MGTO. The proposed layer transforms the features in a manner that is more suitable for classification by spreading the two different class features apart to some extent. When these transformed features are used for training and validation, then the classification layer gets trained well. Finally better performance is achieved when transformed test dataset is categorized by the trained classification layer.

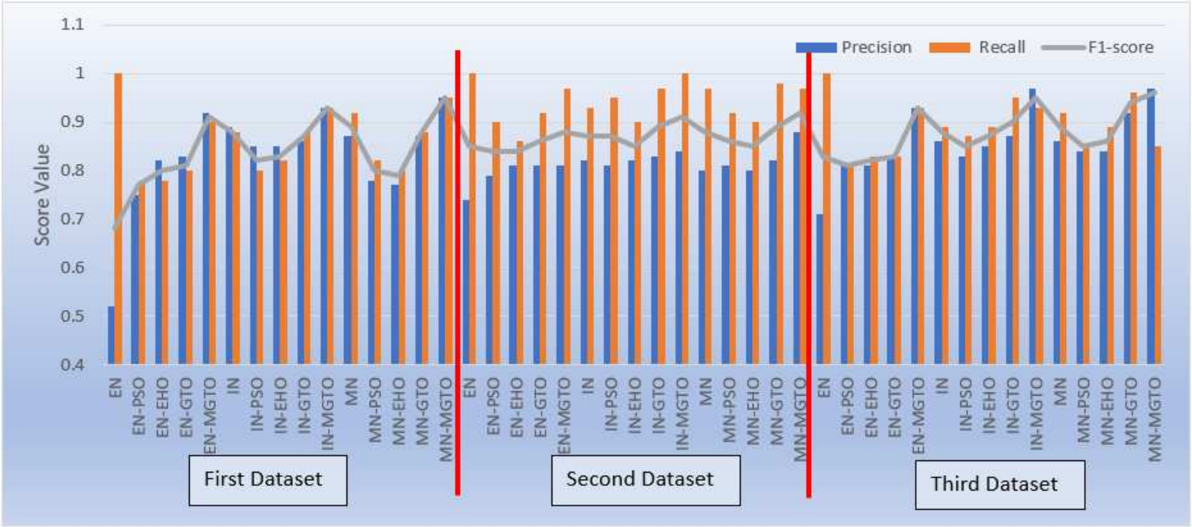

Figure 17. Precision, Recall, and F1 score of various OSCC classification models.

Apart from accuracy, other performance metrics are also relevantly important. Precision gives the percentage of correct OSCC predictions among total number of OSCC predicted. Recall is related to percentage of actual OSCC which was identified correctly as OSCC. F1 score is the harmonic mean of precision and recall score. These metrics are depicted for all the three datasets in Figure 17. Considering these three metrics, DL models with MGTO as intermediate layer outperforms all other investigated intermediate layers. In the first dataset, highest performance is offered by the proposed MobileNetV3-MGTO based DL model through which precision = 0.95, recall = 0.95, and F1-score = 0.95 is achieved. Even on the second and third datasets, highest F1 score is archived by the proposed DL model. Though highest F1 score and accuracy is attained by the proposed DL model on all the three datasets, it fails to attain balanced precision and recall in imbalanced datasets. For example, recall is very much higher than precision for the proposed DL model in second dataset while precision is very much higher than recall for the proposed DL model in third dataset. But it attains almost equal precision and recall in first dataset which is a balanced dataset. Hence wherever higher values of both precision and recall is required on imbalanced dataset, the proposed DL model underperforms there. This could be considered as first limitation of proposed model.

Training time of all the investigated DL models on the first dataset is presented in Table 8. DL models without intermediate layer will get trained comparatively quickly while the presence of intermediate layer may take more training time. MobileNetV3 have less training time since the number of features extracted is 1280 while the number of features extracted by EfficientNetB3 and InceptionNetV2 is 1536. A pie chart is presented in Figure 18 which depicts the percentage of time taken by a DL model when compared to the total training time taken by all the DL models. PSO and EHO takes relatively less training time than other intermediate layers due to their simple structure. When compared to GTO, the proposed MGTO intermediate layer will take more training time due to the inclusion of sine and cosine argument calculations. Only 2% of total training time is taken by MobileNetV3 DL model without any intermediate layer while 7% of total training time is taken by the proposed DL model. This could be considered as second limitation.

Table 8. Time taken for training various DL models.

DL Model	Training Time (hh:mm:ss)	DL Model	Training Time (hh:mm:ss)

MN	00:05:33	IN-EHO	00:18:22
EN	00:15:42	MN-GTO	00:15:15
IN	00:14:37	EN-GTO	00:19:17
MN-PSO	00:09:23	IN-GTO	00:21:39
EN-PSO	00:17:52	MN-MGTO	00:15:52
IN-PSO	00:17:01	EN-MGTO	00:20:12
MN-EHO	00:12:47	IN-MGTO	00:22:21
EN-EHO	00:18:46		

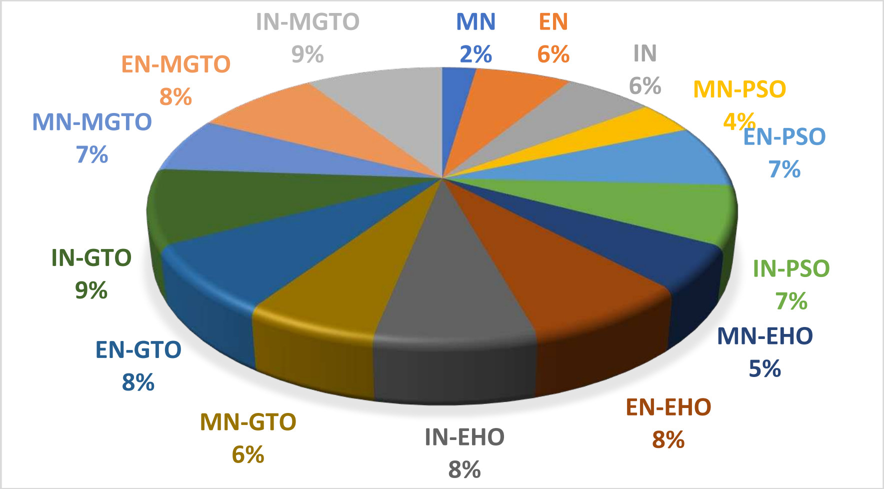

Figure 18. Pie-chart representing the percentage of training time taken by each DL model with respect to total training time taken by all DL models.

The accuracy comparison of some related works for oral cancer detection is presented in Table 9. Supervised classifiers such as K-Nearest Neighbour, Support Vector machine attains comparatively lesser accuracy than the deep learning models. The proposed deep learning model with MGTO as intermediate layer offers the highest accuracy of 95% and shows the importance of proposed DL model.

Table 9. Comparison of accuracy attained in related works.

Related Works	Year	Classification Framework	Accuracy (%) attained
A. U. Rahman et al. [25]	2022	AlexNet	90.06%
M. Aberville [48]	2017	Convolutional Neural Network	88.3%
H. Alkhadar [49]	2021	KNN, Logistic Regression, Decision Tree, Random Forest	76%
A.Alhazmi [50]	2021	Artificial Neural Network	78.95%
C.S. Chu [51]	2020	SVM, KNN	70.59%
R.A.Welikala [52]	2020	ResNet101	78.30%
Shavlokhova, V [53]	2021	CNN	77.89%
Proposed	2023	Pre-trained MobileNetV3 for feature extraction and MGTO as intermediate layer	95%

7. Conclusion

This research work focuses on developing an enhanced deep learning model to diagnose OSCC disease. The proposed DL model with MGTO as intermediate layer and MobileNetV3 as feature extraction layer is able to classify 95% of the histopathological oral images correctly. Totally three oral histopathological images datasets were tested and in all the three datasets, inclusion of MGTO as intermediate layer enhanced the accuracy of DL model. Features were transformed by the MGTO to produce more appropriate features for classification. MGTO outperforms other investigated SI algorithms as an intermediate layer when compared to PSO, EHO, and GTO, primarily due to the modifications made in the GTO equations and its fitness function. The limitations of proposed DL model are relatively higher training time and loss of either precision or recall score in imbalanced dataset. Future work will be in the direction of investigating other SI algorithms as intermediate layer in DL models. In addition, the proposed model needs to be tested for other medical image classification problems.

Funding: This research received no external funding.

Data Availability : The data used for findings will be shared by the author upon request.

Conflicts of Interest: The authors declare no conflict of interest.

References

1. Gupta B., Bray F., Kumar N., Johnson N.W. Associations between oral hygiene habits, diet, tobacco and alcohol and risk of oral cancer: a case–control study from India. Cancer Epidemiol. 2017;51:7–14. doi: 10.1016/j.canep.2017.09.003.
2. Inchingolo, F. et al. Oral cancer: A historical review. Int. J. Environ. Res. Public Health 17, 3168 (2020).
3. Laprise C., Shahul H.P., Madathil S.A., Thekkepurakkal A.S., Castonguay G., Varghese I., Shiraz S., Allison P., Schlecht N.F., Rousseau M.C., Franco E.L., Nicolau B. Periodontal diseases and risk of oral cancer in Southern India: results from the HeNCe Life study. Int. J. Canc. 2016;139:1512–1519. doi: 10.1002/ijc.30201
4. Borse V, Konwar AN, Buragohain P. Oral cancer diagnosis and perspectives in India. Sens Int. 2020;1:100046. doi: 10.1016/j.sintl.2020.100046. Epub 2020 Sep 24. PMID: 34766046; PMCID: PMC7515567.
5. Ajay P., Ashwinirani S., Nayak A., Suragimath G., Kamala K., Sande A., Naik R. Oral cancer prevalence in Western population of Maharashtra, India, for a period of 5 years. J. Oral Res. Rev. 2018;10:11. doi: 10.4103/jorr.jorr_23_17.
6. Karadaghy OA, Shew M, New J, Bur AM. Development and assessment of a machine learning model to help predict survival among patients with oral squamous cell carcinoma. JAMA Otolaryngol Head Neck Surg. 2019;145(12):1115-1120
7. Seoane-Romero J, Vazquez-Mahia I, Seoane J, Varela-Centelles P, Tomas I, Lopez-Cedrun J. Factors related to late stage diagnosis of oral squamous cell carcinoma. Medicina Oral Patología Oral y Cirugia Bucal. 2012;17(1):e35-e40.
8. Dascălu I.T. Histopathological aspects in oral squamous cell carcinoma. Open Access J. Dent. Sci. 2018;3 doi: 10.23880/oajds-16000173
9. Mangalath U., Mikacha M.K., Abdul Khadar A.H., Aslam S., Francis P., Kalathingal J. Recent trends in prevention of oral cancer. J. Int. Soc. Prev. Community Dent. 2014;4:131. doi: 10.4103/2231-0762.149018.
10. N. O'Mahony, S. Campbell, A. Carvalho, S. Harapanahalli, G.V. Hernandez, L. Krpalkova, D. Riordan, J. Walsh, Deep learning vs. traditional computer vision, in: Science and Information Conference, Springer, 2019, pp. 128–144.
11. I.J. Hussein, M.A. Burhanuddin, M.A. Mohammed, N. Benameur, M.S. Maashi, M.S. Maashi, Fully automatic identification of gynaecological abnormality using a new adaptive frequency filter and histogram of oriented gradients (hog), Expert Systems (2021) e12789.
12. Sun, Y., Xue, B., Zhang, M., Yen, G.G., Completely Automated CNN Architecture Design Based on Blocks, (2020) IEEE Transactions on Neural Networks and Learning Systems, 31 (4), art. no. 8742788, pp. 1242-1254.
13. Johner, F.M., Wassner, J. Efficient evolutionary architecture search for CNN optimization on GTSRB (2019) Proceedings - 18th IEEE International Conference on Machine Learning and Applications, ICMLA 2019, art. no. 8999305, pp. 56-61
14. Mozafari, M., Farahbakhsh, R., Crespi, N. A BERT-Based Transfer Learning Approach for Hate Speech Detection in Online Social Media (2020) Studies in Computational Intelligence, 881 SCI, pp. 928-940 doi: 10.1007/978-3-030-36687-2_77
15. Khoh, W.H., Pang, Y.H., Teoh, A.B.J., Ooi, S.Y. In-air hand gesture signature using transfer learning and its forgery attack (2021) Applied Soft Computing, Part A 113, art. no. 108033
16. Seyedali Mirjalili, Seyed Mohammad Mirjalili, Andrew Lewis, Grey Wolf Optimizer, Advances in Engineering Software,Volume 69,2014,Pages 46-61
17. M.M.R. Krishnan, C. Chakraborty, A.K. Ray, Wavelet based texture classification of oral histopathological sections, Int. J. Microsc., Sci. Technol. Appl. Educ. 2 (4) (2010) 897–906.
18. M.M.R. Krishnan, P. Shah, A. Choudhary, C. Chakraborty, R.R. Paul, A.K. Ray, Textural characterization of histopathological images for oral sub-mucous fibrosis detection, Tissue Cell 43 (5) (2011) 318–330

19. M. Krishnan, U. Acharya, C. Chakraborty, A. Ray, Automated diagnosis of oral cancer using higher order spectra features and local binary pattern: a comparative study, Technol. Cancer Res. Treat. 10 (5) (2011) 443–455.
20. R. Patra, C. Chakraborty, J. Chatterjee, Textural analysis of spinous layer for grading oral submucous fibrosis, Int. J. Comput. Appl. 47 (2012) 975–8887.
21. M. M. R. Krishnan, V. Venkatraghavan, U. R. Acharya, M. Pal, R. R. Paul, L. C. Min, A. K. Ray, J. Chatterjee, and C. Chakraborty, ''Automated oral cancer identification using histopathological images: A hybrid feature extraction paradigm,'' Micron, vol. 43, nos. 2–3, pp. 352–364, Feb. 2012.
22. B. Thomas, V. Kumar, and S. Saini, ''Texture analysis based segmentation and classification of oral cancer lesions in color images using ANN,'' in Proc. IEEE Int. Conf. Signal Process., Comput. Control (ISPCC), Sep. 2013, pp. 1–5
23. T. Rahman, L. Mahanta, C. Chakraborty, A. Das, J. Sarma, Textural pattern classification for oral squamous cell carcinoma, J. Microsc. 269 (1) (2018) 85–93.
24. T.Y. Rahman, L.B. Mahanta, A.K. Das, J.D. Sarma, Automated oral squamous cell carcinoma identification using shape, texture and color features of whole image strips, Tissue Cell 63 (2020) 101322.
25. A. U. Rahman, A. Alqahtani, N. Aldhaferi et al., "Histopathologic oral cancer prediction using oral squamous cell carcinoma biopsy empowered with transfer learning," Sensors, vol. 22, no. 10, p. 3833, 2022
26. K. Warin, W. Limprasert, S. Suebnukarn, S. Jinapornthan, and P. Jantana, "Automatic classifcation and detection of oral cancer in photographic images using deep learning algorithms," Journal of Oral Pathology and Medicine, vol. 50, no. 9, pp. 911–918, 2021.
27. S. Camalan, H. Mahmood, H. Binol et al., "Convolutional neural network-based clinical predictors of oral dysplasia: class activation map analysis of deep learning results," Cancers, vol. 13, p. 1291, 2021.
28. J. Musulin, D. Stifani´c, A. Zulijani, T. ˇ Cabov, A. Dekani´c, and ´ Z. Car, "An enhanced histopathology analysis: an AI-based system for multiclass grading of oral squamous cell carcinoma and segmenting of epithelial and stromal tissue," Cancers, vol. 13, p. 1784, 2021.
29. M. Das, R. Dash, and S. K. Mishra, "Automatic detection of oral squamous cell carcinoma from histopathological images of oral mucosa using deep convolutional neural network," International Journal of Environmental Research and Public Health, vol. 20, no. 3, p. 2131, 2023.
30. H. Lin, H. Chen, L. Weng, J. Shao, and J. Lin, "Automatic detection of oral cancer in smartphone-based images using deep learning for early diagnosis," Journal of Biomedical Optics, vol. 26, no. 8, Article ID 086007, 2021.
31. N. Das, E. Hussain, L.B. Mahanta, Automated classification of cells into multiple classes in epithelial tissue of oral squamous cell carcinoma using transfer learning and convolutional neural network, Neural Netw. 128 (2020) 47–60.
32. S. Panigrahi, J. Das, and T. Swarnkar, "Capsule network based analysis of histopathological images of oral squamous cell carcinoma," Journal of King Saud University-Computer and Information Sciences, vol. 34, no. 7, pp. 4546–4553, 2022.
33. H. Myriam, A. A. Abdelhamid, E. S. M. El-Kenawy et al., "Advanced meta-heuristic algorithm based on Particle Swarm and Al-biruni Earth Radius optimization methods for oral cancer detection," IEEE Access, vol. 11, pp. 23681–23700, 2023.
34. Panneerselvam, K., Nayudu, P.P. Improved Golden Eagle Optimization Based CNN for Automatic Segmentation of Psoriasis Skin Images. Wireless Pers Commun 131, 1817–1831 (2023). https://doi.org/10.1007/s11277-023-10522-0
35. Erkan, U., Toktas, A. & Ustun, D. Hyperparameter optimization of deep CNN classifier for plant species identification using artificial bee colony algorithm. J Ambient Intell Human Comput 14, 8827–8838 (2023). https://doi.org/10.1007/s12652-021-03631-w
36. Vinaykumar, V.N., Babu, J.A., Frnda, J."Optimal guidance whale optimization algorithm and hybrid deep learning networks for land use land cover classification" (2023) Eurasip Journal on Advances in Signal Processing, 2023 (1), art. no. 13. doi: 10.1186/s13634-023-00980-w
37. Anilkumar Gona, M. Subramoniam, R. Swarnalatha, Transfer learning convolutional neural network with modified Lion optimization for multimodal biometric system, Computers and Electrical Engineering,Volume 108,2023, 108664, https://doi.org/10.1016/j.compeleceng.2023.108664.
38. Sannasi Chakravarthy S.R., Bharanidharan N., Rajaguru H., Deep Learning-Based Metaheuristic Weighted K-Nearest Neighbor Algorithm for the Severity Classification of Breast Cancer, IRBM, Vol.no.44, issue 3, 2023
39. K. O'Shea and R. Nash, ''An introduction to convolutional neural networks,'' Dec. 2015, arXiv:1511.08458.
40. S.-H. Wang, P. Phillips, Y. Sui, B. Liu, M. Yang, and H. Cheng, ''Classification of Alzheimer's disease based on eight-layer convolutional neural network with leaky rectified linear unit and max pooling,'' J. Med. Syst., vol. 42, no. 5, p. 85, Mar. 2018.

41. C. Szegedy, V. Vanhoucke, S. Ioffe, J. Shlens, Z. Wojna, Rethinking the inception architecture for computer vision, in: Proceedings of the IEEE Conference on Computer Vision and Pattern Recognition, 2016, pp. 2818–2826.
42. A.G. Howard, M. Zhu, B. Chen, D. Kalenichenko, W. Wang, T. Weyand, M. Andreetto, H. Adam, MobileNets: Efficient convolutional neural networks for mobile vision applications, arXiv preprint arXiv:1704.04861, 2017.
43. Mingxing Tan 1 Quoc V. Le, EfficientNet: Rethinking Model Scaling for Convolutional Neural Networks, arXiv:1905.11946v5 [cs.LG] 11 Sep 2020
44. Abdollahzadeh B, Soleimanian Gharehchopogh F, Mirjalili S. Artificial gorilla troops optimizer: A new nature-inspired metaheuristic algorithm for global optimization problems. Int J Intell Syst. 2021;1-72.
45. Gad, A.G. Particle Swarm Optimization Algorithm and Its Applications: A Systematic Review. *Arch Computat Methods Eng* 29, 2531–2561 (2022).
46. Li, J.; Lei, H.; Alavi, A.H.; Wang, G.-G. Elephant Herding Optimization: Variants, Hybrids, and Applications. *Mathematics* 2020, *8*, 1415. https://doi.org/10.3390/math8091415
47. Mirjalili, S. SCA: A sine cosine algorithm for solving optimization problems. Knowl. Based Syst. 2016, 96, 120–133.
48. Aubreville, M.; Knipfer, C.; Oetter, N.; Jaremenko, C.; Rodner, E.; Denzler, J.; Bohr, C.; Neumann, H.; Stelzle, F.; Maier, A. Automatic Classification of Cancerous Tissue in Laserendomicroscopy Images of the Oral Cavity using Deep Learning. Sci. Rep. 2017, 7, 11979.
49. Alkhadar, H.; Macluskey, M.; White, S.; Ellis, I.; Gardner, A. Comparison of machine learning algorithms for the prediction of five-year survival in oral squamous cell carcinoma. J. Oral Pathol. Med. 2021, 50, 378–384
50. Alhazmi, A.; Alhazmi, Y.; Makrami, A.; Salawi, N.; Masmali, K.; Patil, S. Application of artificial intelligence and machine learning for prediction of oral cancer risk. J. Oral Pathol. Med. 2021, 50, 444–450.
51. Chu, C.S.; Lee, N.P.; Adeoye, J.; Thomson, P.; Choi, S.W. Machine learning and treatment outcome prediction for oral cancer. J. Oral Pathol. Med. 2020, 49, 977–985
52. Welikala, R.A.; Remagnino, P.; Lim, J.H.; Chan, C.S.; Rajendran, S.; Kallarakkal, T.G.; Zain, R.B.; Jayasinghe, R.D.; Rimal, J.; Kerr, A.R.; et al. Automated Detection and Classification of Oral Lesions Using Deep Learning for Early Detection of Oral Cancer. IEEE Access 2020, 8, 132677–132693
53. Shavlokhova, V.; Sandhu, S.; Flechtenmacher, C.; Koveshazi, I.; Neumeier, F.; Padrón-Laso, V.; Jonke, Ž.; Saravi, B.; Vollmer, M.; Vollmer, A.; et al. Deep Learning on Oral Squamous Cell Carcinoma Ex Vivo Fluorescent Confocal Microscopy Data: A Feasibility Study. J. Clin. Med. 2021, 10, 5326

Disclaimer/Publisher's Note: The statements, opinions and data contained in all publications are solely those of the individual author(s) and contributor(s) and not of MDPI and/or the editor(s). MDPI and/or the editor(s) disclaim responsibility for any injury to people or property resulting from any ideas, methods, instructions or products referred to in the content.